

Blends · Thermoplastic elastomer · Thermorheological properties · Extrusion · Nitrile rubber · Poly(styrene-co-acrylonitrile)

The present paper reports the results of studies on the thermorheological properties and extrudate characteristics of the 60/40, 70/30 and 80/20 nitrile rubber (NBR)/poly(styrene-co-acrylonitrile) (SAN) blends. The effects of dynamic vulcanization and replacement of a part of the virgin NBR by a nitrile rubber vulcanizate powder (w-NBR) on the 70/30 NBR/SAN blend were also investigated. The blends show pseudoplastic behavior. Replacement of the rubber phase by w-NBR improves the die swell characteristics and surface finish of the extrudates of the thermoplastic elastomeric blend. The blends are 'thermorheologically complex'.

### Thermorheologische Eigenschaften von Thermoplastischen Elastomer-Verschnitten aus NBR/SAN mit Gummimehl aus NBR-Vulkanisaten

Verschnitte · thermoplastische Elastomere · Extrusion · Nitrilkautschuk · SAN

Die Arbeit fasst die Ergebnisse von thermorheologischen Untersuchungen und Versuchen zum Extrusionsverhalten an NBR/SAN-Verschnitten (60/40, 70/30 und 80/20) zusammen. Die Effekte der dynamischen Vulkanisation und der Substitution eines Teils des originären NBR durch Gummimehl aus NBR-Vulkanisaten wurden ebenfalls untersucht. Die Versuche zeigen ein pseudoplastisches Materialverhalten. Durch den Einsatz von NBR-Gummimehl wurden die Spritzquellung und die Oberflächenbeschaffenheit von Extrudaten der Thermoplastischen Elastomerverschnitte verbessert. Die Verschnitte haben ein thermorheologisch komplexes Verhalten.

## Thermorheological Properties of Thermoplastic Elastomeric Blends of NBR/SAN Containing Waste Nitrile Rubber Vulcanizate Powder

A better understanding of the rheological behavior of polymer blends and alloys is essential for controlling the morphology and optimal processing conditions. Polymer blends usually form two or more phases in molten state, a phenomenon that may be attributed to the low entropy of mixing of dissimilar polymers [1]. Han and co-workers [2–4] made experimental studies on the rheological properties of blends of high density poly(ethylene) (HDPE) having widely different molecular weight distributions and poly(styrene)/poly(propylene) blends. They studied the effects of blend ratio on the viscosity and elasticity of blends and their variation with processing variables (i.e., shear rate and melt temperature).

The rheological and viscoelastic properties of multiphase polymer blends show complex behavior due to the difference in the flow behavior of the individual polymers in the blend [5–7]. Viscosity of the components, interfacial interaction between the phases, and the processing parameters are found to influence the morphology of the multiphase polymer blends [8]. Thermoplastic dynamic vulcanizates (TDV), also called elastomer alloy thermoplastic vulcanizates (EA TPV), belong to a novel family of thermoplastic elastomers. TDVs are produced by dynamic crosslinking of blends composed of thermoplastic resins and elastomers [9]. The term "dynamic" or "in-situ" crosslinking means the selective curing of the rubber and its fine dispersion in a molten thermoplastic resin via an intensive mixing and kneading process. This process yields a fine dispersion of partially or fully crosslinked micron size rubber particles in a thermoplastic matrix. The main advantage of TDVs is that they are processable like thermoplastics and they can be recycled without much deterioration in properties [9, 10].

Rheological behavior and extrudate morphology of thermoplastic elastomers

from natural rubber (NR) and high density poly(ethylene) were studied by Akhtar, et al. [11]. Roy and Gupta [12] explored the rheological behavior of short carbon fiber-filled thermoplastic elastomer based on styrene-isoprene-styrene block copolymer. The same authors reported the results of rheological properties of short carbon fiber filled thermoplastic elastomer based on NR/HDPE blends [13]. Naskar, et al. [14, 15] reported thermorheological behavior of the poly(vinyl chloride) (PVC)/maleated ground rubber tire (m-GRT) and PVC/chlorinated GRT (Cl-GRT) blends using parallel plate rheometry. Rheological properties of nylon-6/acrylate rubber (ACM) blends were reported by Jha, et al. [16]. Varughese [17] studied the melt rheology of plasticized PVC/epoxidized NR blends by capillary rheometry. Kader, et al. [18] studied the rheological behavior of acrylate rubber (ACM)/fluoro rubber (FKM) blends using parallel plate rheometry. Ray et al. [19] investigated the rheological behavior of ethylene-octene copolymer [engage] irradiated by electron beam. Jacob, et al. [20] studied the processability of an ethylene-propylene-diene rubber (EPDM) compound containing ground EPDM vulcanizate and observed that addition of ground EPDM causes a decrease in die swell and improved surface smoothness. Ghosh, et al. [21] studied the effects of blend ratio and vulcanizate powders on the processa-



S. Anandhan, P.P. De, S.K. De, A.K. Bhowmick, Kharagpur (India), S. Swayajith, Bangalore (India)

Corresponding author:  
 Anil K. Bhowmick  
 Rubber Technology Center  
 Indian Institute of Technology  
 Kharagpur-72 13 02, India  
 Tel: + 91-32 22-28 31 80;  
 Fax: + 91-32 22-27 71 90  
 E-mail: anilkb@rtc.iitkgp.in



**KGK** RUBBERPOINT

Discover more interesting articles  
and news on the subject!

[www.kgk-rubberpoint.de](http://www.kgk-rubberpoint.de)



Entdecken Sie weitere interessante  
Artikel und News zum Thema!

bility of silicone rubber/fluoro rubber blends.

The effects of mixing sequence and dynamic vulcanization on the mechanical properties of thermoplastic elastomeric NBR/SAN blends have been reported by Anandhan, et al. [22]. The same authors studied the effects of replacement of virgin NBR by waste nitrile rubber powder (w-NBR) in a dynamically vulcanized thermoplastic elastomeric 70:30 NBR/SAN blend [23].

In this paper, the effects of blend ratio on thermorheological properties of NBR/SAN blends are reported. The thermorheological properties of the dynamically vulcanized thermoplastic elastomeric 70:30 NBR/SAN blend containing w-NBR have also been discussed.

## Experimental

### Materials

The details of the materials used are given in *Table 1*.

### Preparation of the waste nitrile rubber vulcanizate powder

A model nitrile rubber vulcanizate powder (w-NBR) was prepared in the laboratory from a precursor vulcanizate sheet based on a standard oil seal formulation: NBR, 100; carbon black N770, 50; DOP (dioctyl phthalate), 5; zinc oxide, 5; stearic acid, 1; IPPD (N-isopropyl p-phenylene diamine), 1; MBTS (mercapto benzothiazole), 1.5; TMTM (tetramethyl thiuram monosulfide), 0.1; sulfur, 1.5; the figures are in phr (that is, parts per hundred parts of rubber, by weight). The rubber compound was prepared in a laboratory size two-roll mill (Schwabenthan, Germany). The optimum curing time of 6.75 minutes at 150 °C was determined by a Monsanto Rheometer MDR 2000. Additional ten minutes were provided for curing of the thick sheets of 9 mm thickness, which were used for preparing the w-NBR powder. The thick sheets of 9 mm thickness were aged at 100 °C in an air-ageing oven for 48 hours and then abraded against a rotating silicon carbide wheel of a mechanical grinder (Ralliwolf TG-6 bench grinder, 2950 rpm) at room temperature. The powder was collected in a holder placed beneath the grinder.

### Preparation of the Blends

The blends were prepared by mixing NBR and SAN in an internal mixer (Brabender Plasticorder PLE 330, Germany) at 180 °C and 60 rpm with cam-type rotors. After

Material	Supplier/Manufacturer
NBR Grade: N553NS ACN content: 34 % Mooney Viscosity: ML <sub>1+4</sub> at 100 °C, 46 M <sub>v</sub> : 2.39 × 10 <sup>5</sup> (viscometry)	Apar Industries Ltd. Mumbai, India.
SAN Grade: Lustron Sparkle ACN content: 27 % M <sub>w</sub> : 1.65 × 10 <sup>5</sup> (GPC) MFI: 1.91 g/10 minutes at 200 °C under a load of 2.16 kg.	Monsanto, St. Louis, MO, USA
Zinc Oxide <sup>a</sup>	E-Merck, Mumbai, India
Stearic acid <sup>a</sup>	Local supplier
IPPD <sup>a, b</sup>	ICI Ltd, Rishra, India
N770 black	Philips Carbon Black Ltd., Durgapur, India
Dioctyl phthalate	Ranbaxy Ltd., Mumbai, India
MBT <sup>a, c</sup>	ICI Ltd., Rishra, India
MBTS <sup>a, d</sup>	ICI Ltd., Rishra, India
TMTM <sup>a, e</sup>	ICI Ltd., Rishra, India
TMTD <sup>a, f</sup>	ICI Ltd., Rishra, India
Sulfur	Qualigens, Mumbai, India

<sup>a</sup> rubber grade <sup>b</sup> N, N'-isopropyl parphenylene diamine (antioxidant) <sup>c</sup> Mercapto benzothiazole (accelerator) <sup>d</sup> Mercapto benzothiazole disulfide (accelerator) <sup>e</sup> Tetramethyl thiuram monosulfide (accelerator) <sup>f</sup> Tetramethyl thiuram disulfide (accelerator)

Description	Mixing equipment and temperature	Mixing time and rpm
(i) NBR charged	Brabender Plasticorder at 70 °C	1 minute at 45 rpm
(ii) Sulfur, zinc oxide, stearic acid and w-NBR added	Brabender Plasticorder at 70 °C	2 minutes at 60 rpm
(iii) Accelerators added.	Two roll mill at 25 °C	2 minutes
(iii) Rubber compound sheeted out and cut to strips	Two roll mill at 25 °C	2 minutes
(iv) SAN softened	Brabender Plasticorder at 180 °C	2 minutes at 30 rpm
(v) Strips of rubber masterbatch added.	Brabender Plasticorder at 180 °C	4 minutes at 60 rpm.
(vi) Blend sheeted out.	Two roll mill at 25 °C	—

mixing, the blends were removed in hot condition and sheeted out in a water-cooled two-roll mill at 25 °C. B<sub>0</sub> and B<sub>10</sub> denote neat SAN and neat NBR respectively. The 60/40, 70/30 and 80/20 (w/w ratio) NBR/SAN blends were denoted as B<sub>6</sub>, B<sub>7</sub> and B<sub>8</sub>. The B<sub>7</sub> blend was dynamically vulcanized. This was shown to possess thermoplastic elastomeric character [22]. For the preparation of the thermoplastic elastomeric 70:30 NBR/SAN blend, the procedure was as follows: NBR was charged in the Brabender Plasticorder at 70 °C. Sulfur, zinc oxide and stearic acid were added. Mixing was done at 60 rpm for 4 minutes. The rubber compound was passed through a two-roll mill. MBT and TMTD were added and the rubber masterbatch was prepared. SAN was softened in the Brabender Plasticorder at 180 °C for 2 minutes. The rubber masterbatch was added to the softened SAN and mixed at 60 rpm for 4 minutes (by which time, the torque stabilized). The mixture was

sheeted out in a two-roll mill and cut into strips. The strips were remixed for 2 minutes in the Brabender Plasticorder and sheeted out in the mill. This blend is designated as W<sub>0</sub>.

The procedure for the preparation of TPE containing w-NBR is shown in *Table 2* and the compound formulations are given in *Table 3*. The control compounds (not dynamically vulcanized) of W<sub>30</sub> and W<sub>45</sub> were also prepared and are designated as W'<sub>30</sub> and W'<sub>45</sub> respectively. The mechanical properties like tensile strength, elongation at break and work to break were determined in a Zwick 1445 UTM at 25 °C according to ASTM D 418-98a by using dumb bell specimens. Tensile testing was done at a cross head speed of 500 mm/min.

The mechanical properties of the control compounds (W'<sub>30</sub> and W'<sub>45</sub>) are given in *Table 4* and it can be seen that dynamic vulcanization improves the mechanical properties.

Ingredients	W <sub>0</sub>	W <sub>20</sub>	W <sub>30</sub>	W <sub>45</sub>
NBR	70	56	49	38.5
w-NBR	0	23.1 (14)	34.7 (21)	52 (31.5)
SAN	30	30	30	30
Zinc oxide	3	3	3	3
Stearic acid	2	2	2	2
MBT	1	1	1	1
TMTD	0.5	0.5	0.5	0.5
Sulfur	0.75	0.75	0.75	0.75

<sup>a</sup> values in parentheses refer to the rubber content in w-NBR.

Mechanical property	W <sub>30</sub>	W <sub>45</sub>	W <sub>30</sub> <sup>a</sup>	W <sub>45</sub> <sup>a</sup>
Tensile strength (MPa)	14.3	15.5	3.0	4.5
Elongation @ break (%)	235	224	48	62
Tension set @ 100% elongation (%)	20	24	a	a
Toughness (Jm <sup>-2</sup> )	9969	10 292	1133	1460

<sup>a</sup> values could not be determined

## Extrudate Characteristics of the Blends

The samples were extruded through an extruder assembly connected to a Brabender Plasticorder PLE 330 at 210 °C at 5, 10, 15, 20 and 30 rpm, which correspond to varying shear rates. The screw had an L/D ratio of 10. The equilibrium die swell defined as the ratio of extrudate diameter to die diameter, was measured after conditioning the samples at room temperature for 48 hours. The diameter of the die was 1 mm. The radius (r) was measured from the mass and density of the samples according to the following formulae [14, 15]:

$$r = [m/(\pi \cdot \rho \cdot h)]^{1/2} \quad (1)$$

where, m, ρ and h are the mass, density and length of the extrudates, respectively. The extrudate surface characteristics were examined by a Scanning Electron Microscope (JSM 5800, JEOL, Peabody, MA, USA) at an accelerating voltage of 20 kV, after sputtering them with gold.

## Results and Discussion

### Effect of Blend Ratio on thermorheological properties

Dynamic shear modulus (G') and complex viscosity (η\*) of the NBR/SAN blends are plotted against various angular frequencies in Figs. 1 and 2 respectively. The G' values increase with increase in frequency. This is due to the fact that at higher frequencies, the polymer molecules get less time to relax. As a result, their stiffness increases.

The sheeted out blends were compression molded between polyester sheets at 210 °C in a hydraulic press (Moore press, Birmingham, UK) at a pressure of 5 MPa for 2 minutes, after which the platens were cooled under pressure. From these molded sheets, discs of 25 mm diameter were punched out and used for rheological studies.

### Parallel Plate Rheometry

Parallel plate rheometry was performed in an ARES rheometer (Advanced Rheometric Expansion System, Rheometric Scientific,

Poole, UK). Dynamic frequency/temperature sweep was performed at 190°, 210°, and 230 °C respectively, and frequency sweep from 0.1 rad/sec to 100 rad/sec at a constant strain amplitude of 1 %. The experiments were performed under a nitrogen atmosphere to avoid decomposition of the samples. Dynamic shear moduli (G' and G'') and complex viscosity (η\*) of the samples were determined as a function of frequency and at different temperatures (190°, 210°, and 230 °C). RSI Orchestrator software was used for data acquisition and analysis.

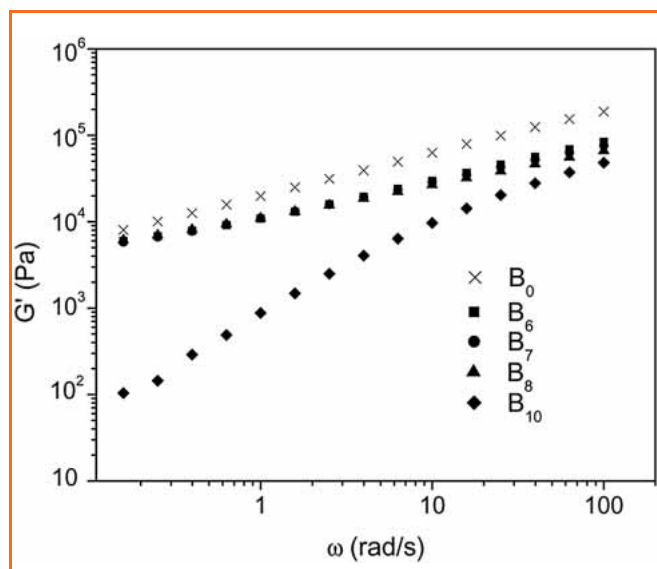


Fig. 1. Dependence of the storage modulus (G') on angular frequency (ω) of NBR, SAN and NBR/SAN blends at 210 °C.

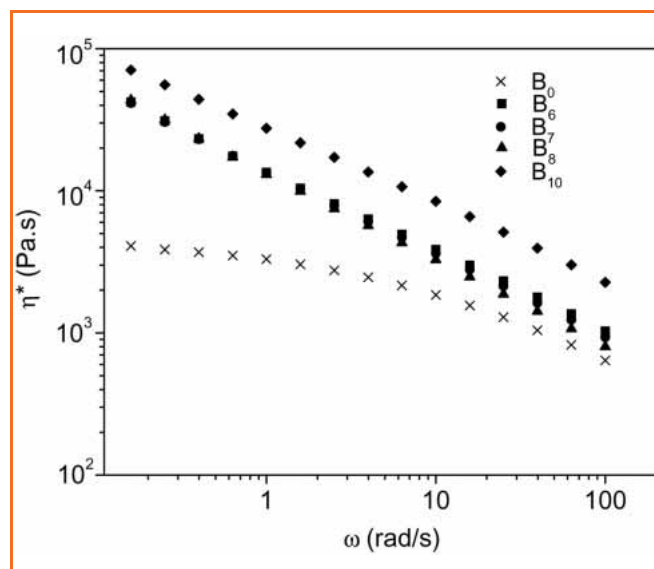


Fig. 2. Dependence of the complex viscosity (η\*) on angular frequency (ω) of NBR, SAN and NBR/SAN blends at 210 °C.

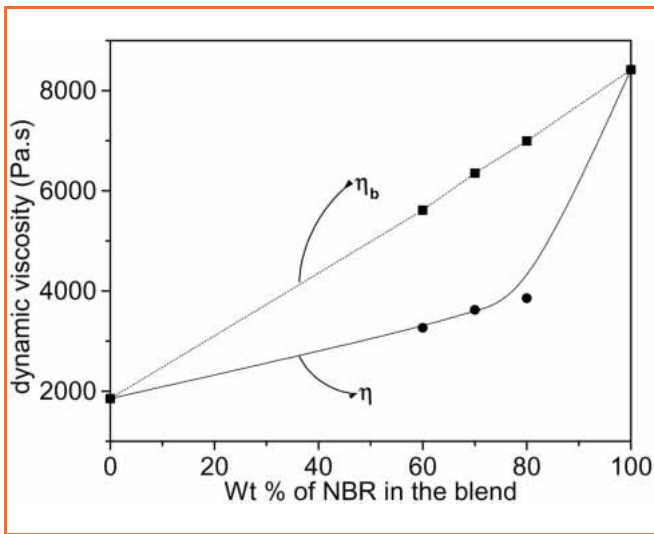


Fig. 3. Variation of theoretical and experimental viscosities with NBR/SAN blend ratio.

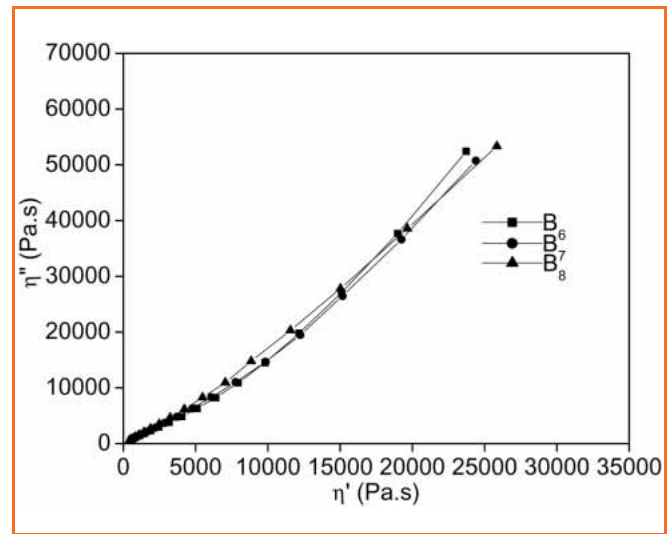


Fig. 4. Cole-Cole plots of the NBR/SAN blends at 210 °C.

The blends show pseudoplastic behavior. Their viscosities decrease with increase in applied frequency, which is a measure of strain rate. The complex viscosity ( $\eta^*$ ) of NBR is higher than that of SAN. Accordingly, the highly viscous NBR forms dispersed phase in a continuous matrix of SAN up to a blend ratio of 60:40 of NBR/SAN, beyond which the morphology changes to a co-continuous one [22].

It has been reported that the viscosity of a polymer blend can be described by using the log additive principle [24].

$$\ln \eta_b = \sum w_i \ln \eta_i \quad (2)$$

where,  $w_i$ ,  $\eta_i$  and  $\eta_b$  are the weight fraction, viscosity of each blend component, and viscosity of the blend, respectively. Theoretical values of viscosity at a constant frequency of 10 rad/s were evaluated for the blends. The deviation in viscosity of blends ( $\Delta \eta$ ) at a given temperature and frequency can be expressed as [25]

$$\Delta \eta = \eta - \eta_b \quad (3)$$

It can be observed that for different blend ratios, the theoretical and experimental viscosity values differ consistently (Fig. 3). A negative deviation from the theoretical viscosity suggests that the blend components NBR and SAN are mutually immiscible as proved by the DMTA and DSC results [22]. The solubility parameters ( $\delta$ ) of NBR [ $\delta_{\text{NBR}} = 19.9 \text{ (J/cc)}^{1/2}$ ] and SAN [ $\delta_{\text{SAN}} = 20.3 \text{ (J/cc)}^{1/2}$ ] (evaluated by Small's method [26]).

The compatibility between the phases can be studied by understanding the complex viscosity function comprising of viscous and elastic components [24, 27].

$$\eta^* = \eta' - i \eta'' \quad (4)$$

where,  $\eta'$  is the in-phase elastic component and  $\eta''$  is the out-of-phase viscous component of the dynamic complex viscosity ( $\eta^*$ ). Moreover, these components are related to the energy stored and the oscillatory frequency by the following equations [14, 15]:

$$\eta' = G''/\omega \text{ and } \eta'' = G'/\omega \quad (5)$$

where,  $G'$  is the storage modulus (elastic component) and  $G''$  is the loss modulus (viscous component) and  $\omega$  is angular frequency. It is also well known that the representation of dynamic shear data or viscosity data in Cole-Cole plot gives information about the relaxation processes taking place in the multiphase blends [24]. It is assumed that when a blend is miscible, the Cole-Cole plot gives almost semicircular curve and we can deduce the average relaxation time of a phase, which is equal to the inverse of the maximal frequency corresponding to the horizontal tangent at the top of the arc. This plot can also be used to determine the zero shear viscosity  $\eta_0$  (obtained from the extrapolation of

Cole-Cole plot to x axis,  $\eta'$  at  $\eta'' = 0$ ). The present systems do not show the characteristics of a semicircular curve (Fig. 4) due to complex temperature and shear rate dependent rheological behavior.

The log-log plots of  $G'$  versus  $G''$  (Han plot) [28, 29] of  $B_6$ ,  $B_7$  and  $B_8$  at different temperatures are given in Fig. 5. It is observed that the Han plots of the blends are dependent of the temperature. Therefore, these blends are thermorheologically complex. It indicates that the melts are not homogeneous at three different temperatures (190°, 210°, and 230 °C).

The relation between complex viscosity ( $\eta^*$ ) and the frequency ( $\omega$ ) can be expressed by the power law given by [14, 15]

$$\eta^* = k(\omega)^{n-1} \quad (6)$$

where,  $\eta^*$  is the complex dynamic viscosity,  $k$  is the power law coefficient and  $n$  is the pseudoplasticity index. The power law coefficients ( $k$ ) and pseudoplasticity index ( $n$ ) values for the blends  $B_6$ ,  $B_7$  and  $B_8$  at different temperatures obtained from the log-log plots of  $\eta^*$  against  $\omega$ , are shown in Table 5. For these blends, pseudoplasticity

Table 5. 'k' and 'n' values of the blends

Sample designation	$k \times 10^4 \text{ (Pa.s}^n\text{)}$			n		
	190 °C	210 °C	230 °C	190 °C	210 °C	230 °C
$B_0$	5.99	4.00	2.77	0.473	0.459	0.429
$B_6$	1.62	1.42	1.35	0.452	0.431	0.377
$B_7$	1.49	1.38	1.29	0.430	0.416	0.359
$B_8$	1.42	1.35	1.28	0.400	0.384	0.350
$B_{10}$	0.89	0.29	0.11	0.624	0.737	0.802
$W_0$	6.89	6.66	6.32	0.133	0.118	0.098
$W_{20}$	3.79	3.68	3.61	0.144	0.131	0.109
$W_{30}$	2.35	2.05	1.88	0.158	0.145	0.130
$W_{45}$	2.68	2.30	2.10	0.165	0.156	0.134



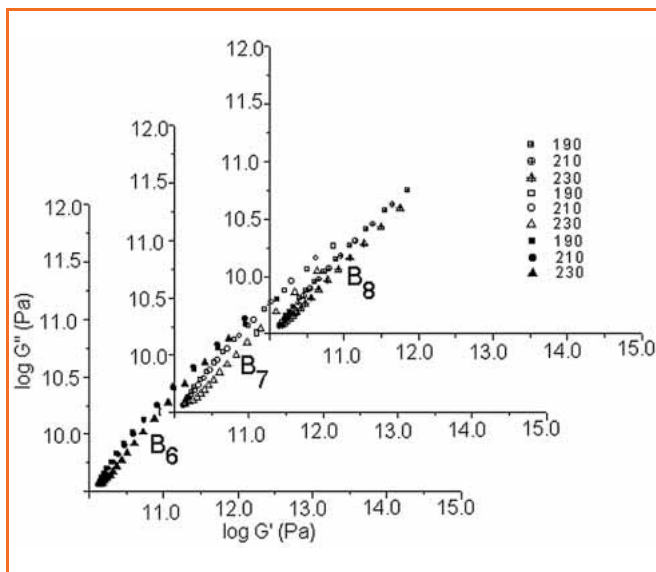


Fig. 5. Han plots of the NBR/SAN blends.

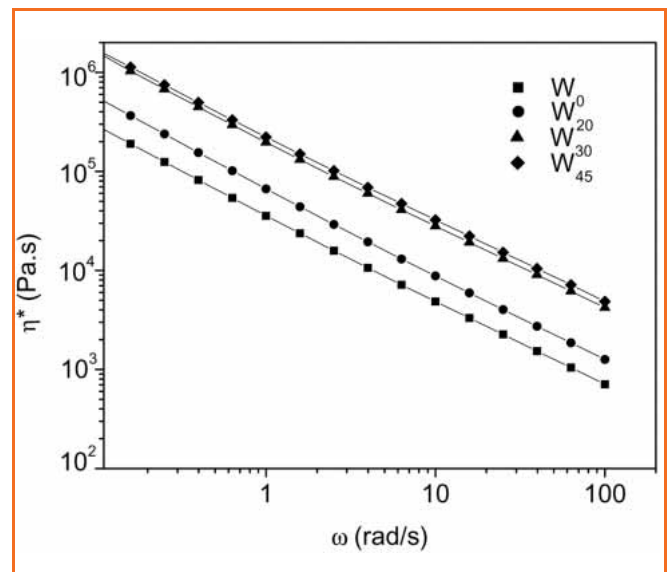


Fig. 6. Dependence of the storage modulus ( $G'$ ) on angular frequency ( $\omega$ ) of the TPE containing w-NBR at 210 °C.

city index ( $n$ ) decreases with increase in temperature. Power law coefficient ( $k$ ), which is a measure of viscosity at unit frequency, decreases with temperature. As the NBR content of the blends increases, the  $k$  and  $n$  values decrease.

### Effect of addition of w-NBR on thermorheological behavior of the thermoplastic elastomer based on NBR/SAN

The plots of dynamic shear modulus ( $G'$ ) versus frequency ( $\omega$ ) are shown in Fig. 6 for the blends  $W_0$ ,  $W_{20}$ ,  $W_{30}$  and  $W_{45}$ . The  $G'$  values of  $W_{20}$ ,  $W_{30}$  and  $W_{45}$  are higher than that of  $W_0$ . This is due to the fact that the filler present in w-NBR reinforces the blends. w-NBR contains aged NBR along with filler and other ingredients. The filler component in w-NBR reinforces the virgin NBR in the blends [23].

The blends display pseudoplastic behavior. The dynamic complex viscosities ( $\eta^*$ ) decrease with increasing frequency which is a measure of shear rate (Fig. 7). The viscosity of the thermoplastic elastomeric blend increases by the addition of w-NBR. The increase in viscosity is due to the presence of solid particles and reinforcing effect of the filler present in w-NBR. The log of complex viscosity ( $\eta^*$ ) at 100 rad/s as a function of w-NBR content is plotted in Fig. 8. Log  $\eta^*$  varies linearly with w-NBR content as evident from Fig. 8.

The log-log plots of  $G'$  versus  $G''$  (Han plot) [28, 29] of  $W_0$ ,  $W_{20}$ ,  $W_{30}$  and  $W_{45}$  at different temperatures are given in

Fig. 9. It is observed from the Han plots of the blends that these blends are 'thermorheologically complex'. It is also found that at all temperatures the TPE compositions containing w-NBR exhibit higher  $G'$  and  $G''$  than that of  $W_0$ . As explained earlier, this is due to the reinforcing effect of the filler present in w-NBR.

The Cole-Cole plots of  $W_0$ ,  $W_{20}$ ,  $W_{30}$  and  $W_{45}$  (Fig. 10) reveal that the nature of

these plots does not change on partial replacement of NBR by w-NBR.

The power law coefficients ( $k$ ) and pseudoplasticity index ( $n$ ) values are given in Table 5. There is a decrease in the  $n$  values with increase in temperature. Power law coefficient ( $k$ ) also decreases.

The activation energies of flow ( $E_f$ ) of the blends are measured from the slope of the natural logarithmic plot of complex visco-

Table 6. Activation energy ( $E_f$ ) values of the NBR/SAN blends

Sample designation	$E_f$ (kJ/mol)	
	10 rad/sec	100 rad/sec
B <sub>6</sub>	136.5	32.9
B <sub>7</sub>	124.2	21.0
B <sub>8</sub>	110.2	15.1
W <sub>0</sub>	144.3	21.3
W <sub>20</sub>	787.3	72.3
W <sub>30</sub>	1056.3	138.2
W <sub>45</sub>	1324.9	176.3

Table 7. Equilibrium die swell values of NBR/SAN blends

Rotor speed (rpm)	B <sub>0</sub>	B <sub>6</sub>	B <sub>7</sub>	B <sub>8</sub>	B <sub>10</sub>
5	1.58	1.55	1.70	1.38	1.52
10	1.74	1.58	1.68	1.43	1.52
15	1.72	1.63	1.70	1.61	1.61
20	1.79	1.64	1.62	1.66	1.60
30	1.95	1.86	1.81	1.76	1.57

Table 8. Equilibrium die swell values of the 70/30 NBR/SAN blend containing w-NBR

Rotor speed (rpm)	W <sub>0</sub>	W <sub>20</sub>	W <sub>30</sub>	W <sub>45</sub>	W' <sub>30</sub>	W' <sub>45</sub>
5	1.35	1.10	1.10	1.13	1.24	1.14
10	1.59	1.09	1.11	1.10	1.32	1.14
15	1.58	1.12	1.15	1.10	1.34	1.18
20	1.63	1.17	1.15	1.12	1.34	1.16
30	1.74	1.18	1.13	1.16	1.32	1.16

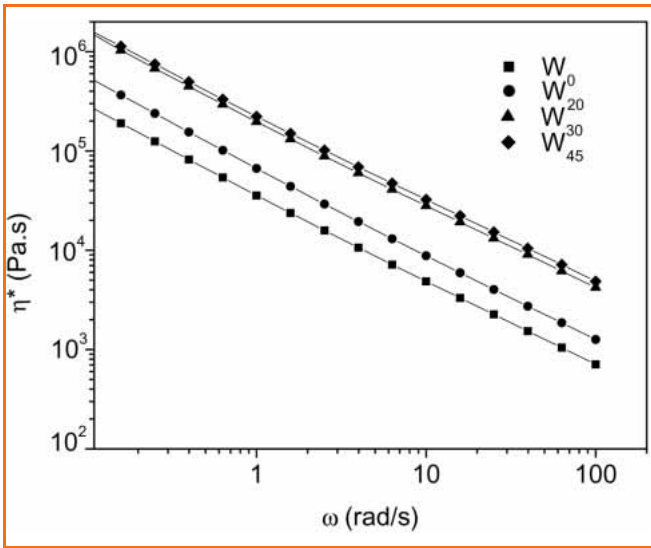


Fig. 7. Dependence of the complex viscosity ( $\eta^*$ ) on angular frequency ( $\omega$ ) of the TPE containing w-NBR at 210°C.

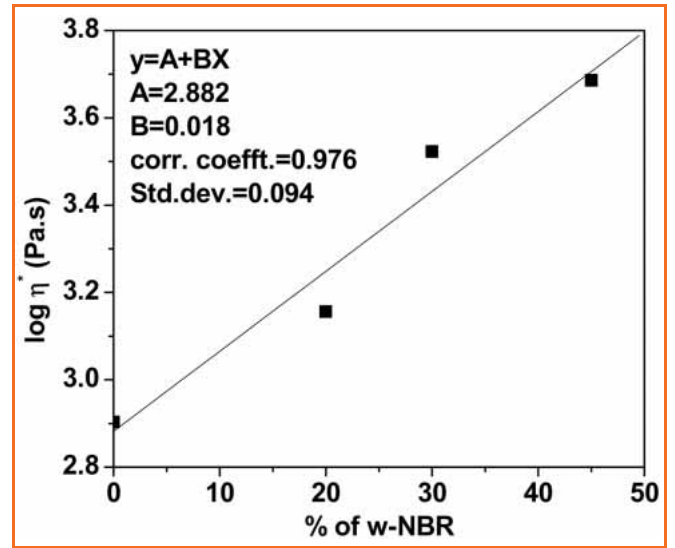


Fig. 8. Log of Complex viscosity ( $\eta^*$ ) of the TPE compositions as a function of w-NBR content at 100 rad/s.

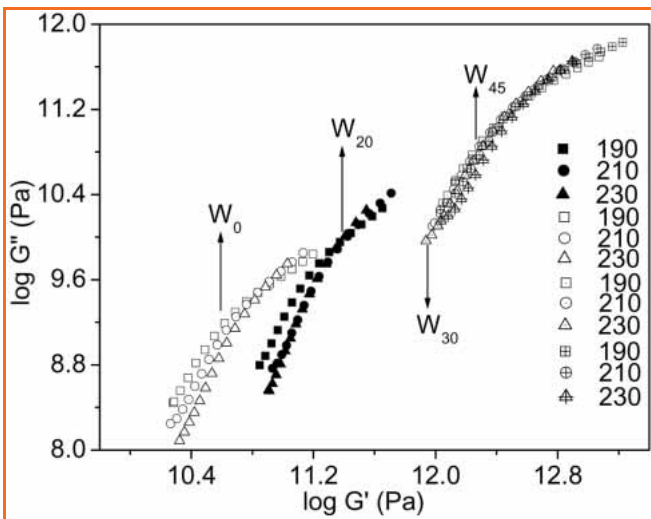


Fig. 9. Log-log plot of  $G'$  versus  $G''$  for the TPE compositions containing w-NBR.

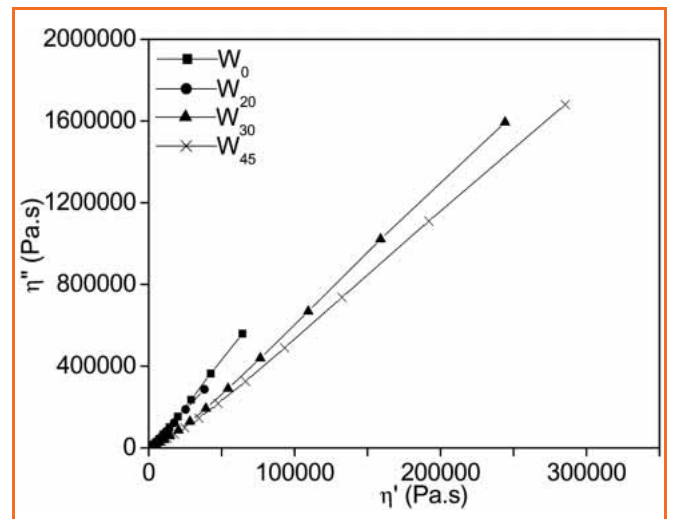


Fig. 10. Cole-Cole plots of the TPE compositions containing w-NBR at 210°C.

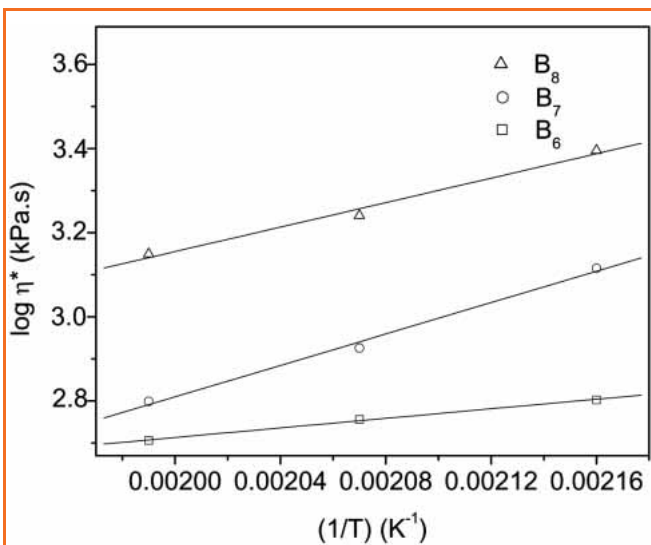


Fig. 11. a) Arrhenius plots of the NBR/SAN blends at 10 rad/s.

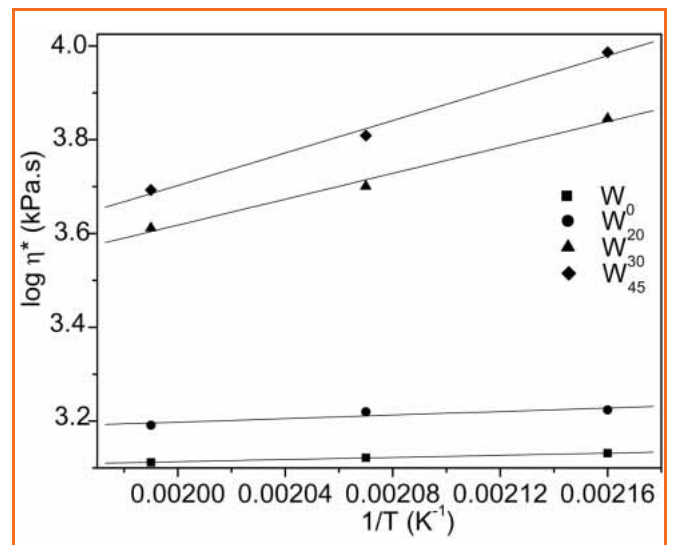


Fig. 11. b) Arrhenius plots of the TPE containing w-NBR at 10 rad/s.

sity at fixed frequency against reciprocal of absolute temperature according to the Arrhenius equation [31]

$$\eta^* = A \cdot \exp(E_f/RT) \quad (7)$$

where, A is an arbitrary constant, T is the absolute temperature and  $R = 8.314 \text{ J K}^{-1} \text{ mol}^{-1}$ .

The Arrhenius plots of the blends – B series ( $B_6$ ,  $B_7$  and  $B_8$ ) and W series ( $W_0$ ,  $W_{20}$ ,  $W_{30}$  and  $W_{45}$ ) at 10 rad/s are shown in Figs. 11 (a) and (b) respectively. It is observed that slope for the blends containing w-NBR is higher than that of  $W_0$ . Incorporation of w-NBR causes an increase in the viscosity of the blend. At higher temperature, viscosity decreases significantly [as observed in Fig. 11 (b)]. Therefore, the activation energy for the w-NBR filled compound is higher than that of  $W_0$ . As the amount of w-NBR increases, the activation energy of flow increases. The activation energies at frequencies 10 rad/s and 100 rad/s are given in Table 6. At higher frequency, flow is facilitated by increased strain rate, causing decrease in  $E_f$  value.

### Extrudate characteristics

The die swell (or swelling ratio) values of the NBR/SAN blends extruded at 5, 10, 15, 20 and 30 rpm and 210 °C are given in Table 7. The die swell values increase with an increase in rpm of the screw. The die swell values of  $B_6$  and  $B_7$  are higher than that of  $B_8$ . The die swell values of the 70/30 NBR/SAN blend containing different amounts of w-NBR are given in Table 8. The die swell values of the 70/30 NBR/SAN blend containing w-NBR are less than that of the control. The carbon black present in w-NBR causes reduction in die swell of the extrudates of rubbers [30, 31].

The SEM photomicrographs showing the extrudate surfaces of  $B_0$ ,  $B_6$ ,  $B_7$ ,  $B_8$  and  $B_{10}$  are given in Figs. 12 (a)–(e) respectively. The extrudate surfaces of  $B_6$ ,  $B_7$ , and  $B_8$  are rough and have the shape of a screwed thread. This phenomenon is known as ‘bambooning’ [30]. This is due to the elastic nature of the melt of these blends and this elastic effect in turn causes melt fracture. The SEM photomicrographs showing the extrudate surfaces of  $W_0$ ,  $W_{20}$ ,  $W_{30}$ ,  $W_{45}$ ,  $W'_{30}$  and  $W'_{45}$  are shown in Figs. 13 (a)–(f). The extrudate surfaces of  $W_{20}$ ,  $W_{30}$ ,  $W_{45}$  are smoother compared to that of  $W_0$ . The filler present in w-

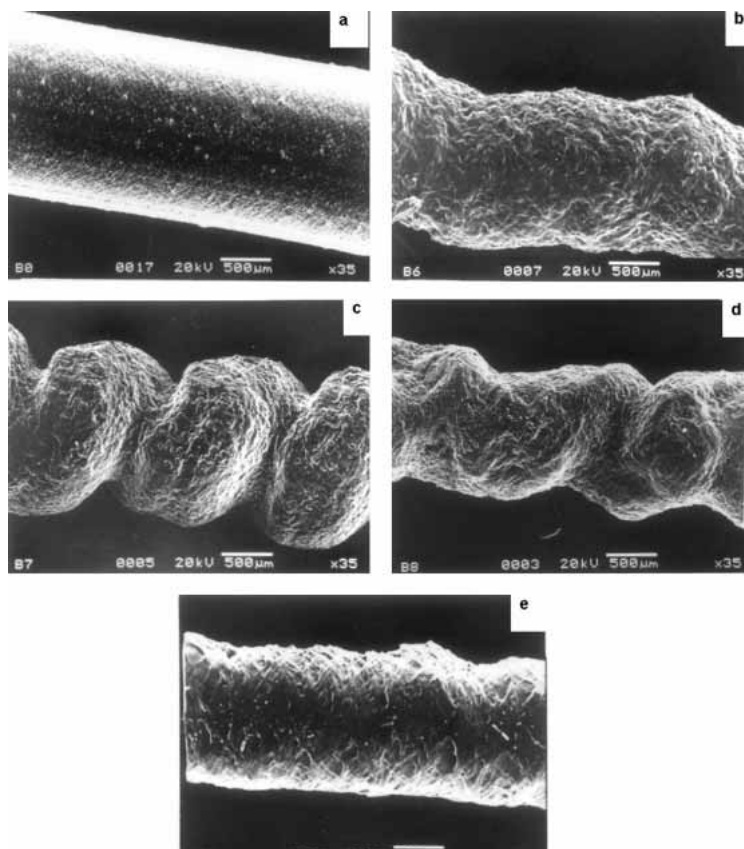


Fig. 12. SEM photomicrographs of the extrudates of (a)  $B_0$ ; (b)  $B_6$ ; (c)  $B_7$ ; (d)  $B_8$  and (e)  $B_{10}$ .

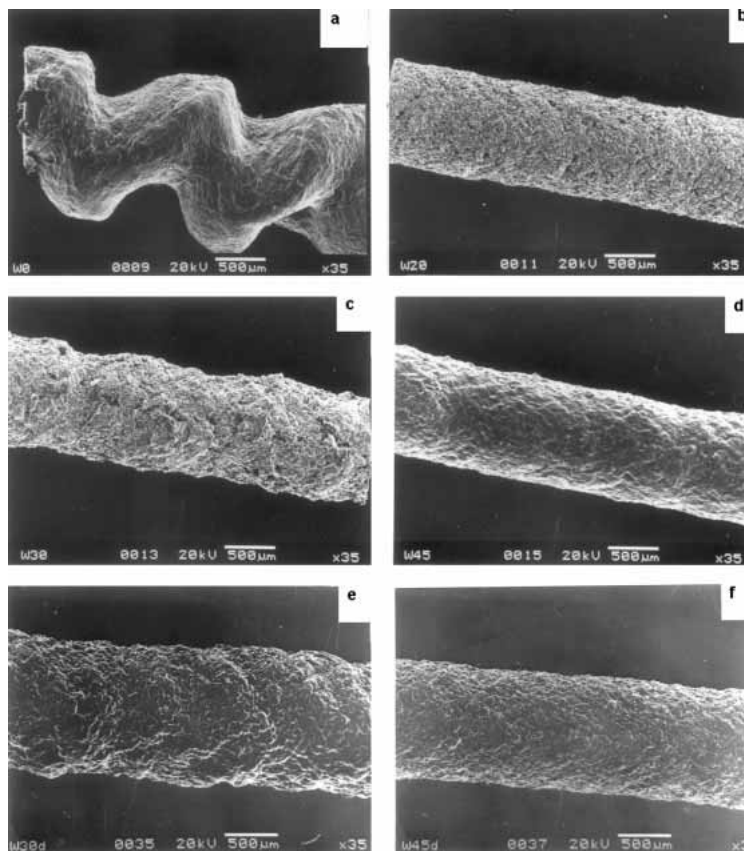


Fig. 13. SEM photomicrographs of the extrudates of (a)  $W_0$ ; (b)  $W_{20}$ ; (c)  $W_{30}$ ; (d)  $W_{45}$ ; (e)  $W'_{30}$  and (f)  $W'_{45}$ .



NBR reduces the elastic turbulence of the melts and hence the surfaces of the blend containing w-NBR are smoother. In order to understand the effect of dynamic cross-linking vis-à-vis filler effect, comparison of  $W_{30}$  with  $W'_{30}$  and  $W_{45}$  with  $W'_{45}$ , reveals that the surfaces are smooth and there is no noticeable effect of dynamic crosslinking on surface smoothness. Therefore, the surface smoothness can be ascribed to the filler effect.

### Conclusions

- 1) The 60/40, 70/30 and 80/20 NBR/SAN blends and the 70/30 NBR/SAN TPE compositions containing w-NBR exhibit pseudoplastic behavior.
- 2) Cole-Cole plots of the NBR/SAN blends and the TPE composition containing w-NBR are characteristic of immiscible blends.
- 3) The flow behavior of these blends obeys power-law model and the blends show deviation from Newtonian behavior.
- 4) The blends are 'thermorheologically complex'.
- 5) Die swell of the NBR/SAN blends with and without w-NBR increases with increasing shear rates. w-NBR reduces the die swell of the thermoplastic elastomeric blends due to the filler effect and improves the surface smoothness.

### Acknowledgement

The authors are grateful to the Department of Science and Technology, Government of India, New Delhi, for sponsoring the project.

### References

[1] P.F. Flory, Principles of Polymer Chemistry, Cornell Univ. Press, Ithaca, New York, 1953.  
 [2] C.D. Han, J. Appl. Polym. Sci. **15** (1971) 2579.  
 [3] C.D. Han and T.C. Yu, J. Appl. Polym. Sci. **15** (1971) 1163.  
 [4] C.D. Han, J. Appl. Polym. Sci. **18** (1974) 481.  
 [5] P. Piersoni, D. Ercoli, G. Goizueta and N. Capati, J. Reinforced Plast. Composite **20** (2001) 182.

[6] Z. Krulis and I. Fortelny, Eur. Polym. J. **33** (1997) 513.  
 [7] C. Liu, J. Wang and J. He, Polymer **43** (2002) 3811.  
 [8] S.Y. Hobbs, M.E. Dekkers and V.H. Watkins, Polymer **29** (1988) 1598.  
 [9] A.K. Bhowmick, H.L. Stephens, Eds, Handbook of Elastomers, 2<sup>nd</sup> Ed, Marcell Dekker, New York, 2001, pp 249–312.  
 [10] A.Y. Coran, Rubber Chem. Technol. **54** (1981) 892.  
 [11] S. Akhtar, B. Kuriakose, P.P. De and S.K. De, Plast. Rubber Proc. Appl. **7** (1987) 11.  
 [12] D. Roy and B.R. Gupta, J. Appl. Polym. Sci. **49** (1993) 1475.  
 [13] D. Roy, A.K. Bhattacharya and B.R. Gupta, J. Elast. Plast. **25** (1993) 46.  
 [14] A.K. Naskar, A.K. Bhowmick, D.P. Gala and S.K. De, Polym. Eng. Sci. **41** (2001) 1087.  
 [15] A.K. Naskar, D.P. Gala, S.K. De and A.K. Bhowmick, Kautsch. Gummi. Kunst. **55** (2002) 164.  
 [16] A. Jha, A.K. Bhattacharya and A.K. Bhowmick, Polymer Networks and Blends **7** (1997) 177.  
 [17] K.T. Varughese, J. Appl. Polym. Sci. **39** (1990) 205.  
 [18] M.A. Kader, D.P. Gala and A.K. Bhowmick, Polym. Eng. Sci. **43** (2003) 975.  
 [19] S. Ray, S. Swayajith and A.K. Bhowmick, J. Appl. Polym. Sci. **90** (2003) 2453.  
 [20] C. Jacob, A.K. Bhattacharya, A. K. Bhowmick, P. P. De and S.K. De, J. Appl. Polym. Sci. **87** (2003) 2204.  
 [21] A. Ghosh, B. Kumar, A. K. Bhattacharya and S.K. De, J. Appl. Polym. Sci. **88** (2003) 2377.  
 [22] S. Anandhan, P.P. De, S.K. De and A.K. Bhowmick, J. Appl. Polym. Sci. **88** (2003) 1976.  
 [23] S. Anandhan, P.P. De, A.K. Bhowmick, S.K. De and S. Bandyopadhyay, J. Appl. Polym. Sci. **90** (2003) 2348.  
 [24] J.D. Ferry, Viscoelastic Properties of Polymers, Wiley, New York, (1980).  
 [25] B. Kumar, S.K. De, A.K. Bhowmick and P.P. De, Polym. Eng. Sci. **42** (2002) 2306.  
 [26] D.W. Van Krevelen, Properties of Polymers, Elsevier, Amsterdam, (1997).  
 [27] Y.J. Kim, G.S. Shin, I.T. Lee and B.K. Kim, J. Appl. Polym. Sci. **47** (1993) 295.  
 [28] P.K. Han and J.L. White, Rubber Chem. Technol. **68** (1995) 728.  
 [29] C.D. Han and M. Jhon, J. Appl. Polym. Sci. **32** (1986) 3809.  
 [30] J.L. White, in Science and Technology of Rubber, F.R. Eirich, Ed., Academic press, New York, (1978).  
 [31] J.A. Brydson, Flow properties of Polymer melts, 2<sup>nd</sup> edition, George Goodwin Ltd., London, (1981).